

Inverse Faraday effect in Mott insulators

Saikat Banerjee^{1,*}, Umesh Kumar¹, and Shi-Zeng Lin^{2,†}¹Theoretical Division, T-4, Los Alamos National Laboratory, Los Alamos, New Mexico 87545, USA²Theoretical Division, T-4 and CNLS, Los Alamos National Laboratory, Los Alamos, New Mexico 87545, USA

(Received 4 September 2021; revised 17 May 2022; accepted 18 May 2022; published 31 May 2022)

The inverse Faraday effect (IFE), where a static magnetization is induced by circularly polarized light, offers a promising route to ultrafast control of spin states. Here we study the IFE in Mott insulators using the Floquet theory. We find two distinct IFE behavior governed by the inversion symmetry. In the Mott insulators with inversion symmetry, we find that the effective magnetic field induced by the IFE couples ferromagnetically to the neighboring spins. While for the Mott insulators without inversion symmetry, the effective magnetic field due to IFE couples antiferromagnetically to the neighboring spins. We apply the theory to the spin-orbit coupled single- and multi-orbital Hubbard model that is relevant for the Kitaev quantum spin liquid material and demonstrate that the magnetic interactions can be tuned by light.

DOI: [10.1103/PhysRevB.105.L180414](https://doi.org/10.1103/PhysRevB.105.L180414)

Introduction. The optical control and manipulation of the magnetic exchange interaction in quantum materials have always been an important centerpiece in condensed matter physics [1,2]. The origin of such magneto-optical studies dates back to Faraday who discovered that the plane of light polarization rotates due to the intrinsic magnetization in a material [3]. Almost a century later, it was predicted [4] and subsequently observed [5] that a circularly polarized light can also generate static magnetic moments. This opposite phenomenon is known as the inverse Faraday effect (IFE), which offers a natural pathway to the ultrafast manipulation of magnetic order in quantum materials [6,7]. Over the past few decades, IFE has remained an active area of research and has been observed in a large class of materials ranging from insulating magnets [6] to nonmagnetic metals [8,9].

However, despite significant experimental progress, the microscopic origin of the IFE has remained relatively unclear from a theoretical point of view. Most of the previous attempts in this direction relied on semiclassical analysis [4,10–12]. Earlier theoretical work by Battiato *et al.* [13] provided a detailed quantum mechanical analysis of metallic IFE, relying on the electronic orbital degrees of freedom. Recently, IFE has been predicted in spin-orbit coupled (SOC) Rashba metals [14], semimetals [15–17], and also for superconductors [18,19]. While the realization of IFE using ultrafast control of spin dynamics in rare-earth orthoferrites [ReFeO₃, Re = Dy, Ho, Er (antiferromagnetic insulator)] has been reported in previous works [6,20–25], a detailed microscopic analysis of the latter in the Mott insulating regime is still lacking.

In this work, we consider a periodically driven Mott insulator in the presence of circularly polarized light and analyze the emergent magnetic field in the Floquet regime. We explore both single- and multi-orbital models and find that the IFE leads to both antiferromagnetic and

ferromagnetic magnetization depending on the inversion symmetry. We employ the time-dependent Schrieffer-Wolff (SW) unitary transformations to derive low-energy spin Hamiltonians. In this case, the transition matrix elements between high-energy (charge excitations) and low-energy states (spin excitations) are removed perturbatively [26–29]. We consider *d*-electron systems with both direct and indirect hopping. The indirect hopping is typically assumed to be mediated through a ligand atom [see Fig. 1]. We show that such ligand-mediated hopping in the presence of SOC gives rise to the IFE. In materials with inversion symmetry, such IFE favors a ferromagnetic state; in contrast, the system without inversion symmetry favors antiferromagnetism.

Symmetry considerations. Before moving on to the microscopic model calculation, here we investigate the IFE based on symmetry considerations. In Mott insulators, the charge degrees of freedom are gapped, and the system can be described in terms of spin degrees of freedom. The direct Zeeman coupling of the electromagnetic fields to spins is much weaker than the orbital coupling and therefore is neglected here; then, the SOC is an essential ingredient for the IFE. Furthermore, the time-reversal symmetry (TRS) must be broken. We consider a minimal hopping path shown in Fig. 1(b) for electrons to experience the TRS breaking laser field, where only the in-plane electric-field components couple to the electron hopping. The minimal coupling between the laser electric field and the system's *static* magnetization has the form $\mathcal{L} = \epsilon_{\alpha\beta\gamma} E_{\alpha}(\Omega) E_{\beta}(-\Omega) M_{\gamma}$, where summation over repeated indices is implied, and Ω is the frequency of the applied laser. Here $\epsilon_{\alpha\beta\gamma}$ is a tensor, and the *static* magnetization is a function of two spin moments in Fig. 1(b), i.e., $M_{\gamma}(\mathbf{S}_1, \mathbf{S}_2)$, whose form is dictated by the symmetries. The whole system of laser and the Mott insulator has TRS, which enforces $\epsilon_{\alpha\beta\gamma} = -\epsilon_{\beta\alpha\gamma}$.

In inversion symmetric systems, the atomic SOC is responsible for the IFE. We consider that the system is also symmetric with respect to the mirror plane of the ions (we call it the *xy* plane with the *z* axis perpendicular to it). This

*saikatb@lanl.gov

†szl@lanl.gov

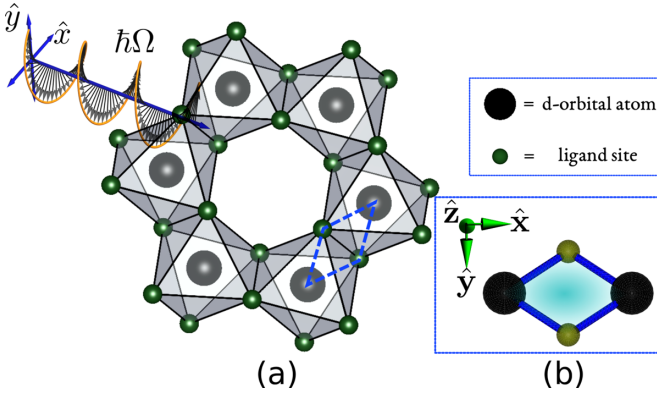


FIG. 1. (a) A schematic of the lattice with edge-sharing octahedral geometry where both the direct (t_{dd}) and the indirect (t_{pd}) hopping amplitudes get modified under the influence of applied circularly polarized light. (b) The four-site cluster [highlighted in panel (a)] including two d orbitals and two ligand atoms, respectively, generates an effective static magnetic field in the presence of circularly polarized light with energy $\hbar\Omega$ (IFE).

restricts $\epsilon_{\alpha\beta\gamma} \neq 0$ only when $\gamma = z$. The inversion symmetry requires that $\mathbf{M} = \hat{\mathbf{z}} \cdot (\mathbf{S}_1 + \mathbf{S}_2)$ with $\hat{\mathbf{z}}$ a unit vector normal to the hopping plane. In this case, the IFE can be written as $\mathcal{L} \propto [\mathbf{E}(\Omega) \times \mathbf{E}^*(\Omega)] \cdot (\mathbf{S}_1 + \mathbf{S}_2)$ [here $\mathbf{E}^*(\Omega) = \mathbf{E}(-\Omega)$], which is the same as IFE for the isotropic medium [4].

The SOC can also arise due to inversion symmetry breaking, which can be described by vector $\boldsymbol{\alpha}$. The direction of $\boldsymbol{\alpha}$ is constrained by other symmetries such as rotation and mirror [30]. We consider symmetry transformations, such as inversion and mirror operation, that include the transformation of $\boldsymbol{\alpha}$, which leaves the \mathcal{L} invariant. The simplest form that is invariant under these transformations is the scalar $M_z = \boldsymbol{\alpha} \cdot (\mathbf{S}_1 - \mathbf{S}_2)$. Here M_z must be proportional to $\mathbf{S}_1 - \mathbf{S}_2$, because $\boldsymbol{\alpha}$ is odd under the inversion transformation $1 \leftrightarrow 2$. The IFE favors the antiferromagnetic arrangement of \mathbf{S}_1 and \mathbf{S}_2 , in contrast with a ferromagnetic arrangement in the inversion symmetric case. This is rather surprising given that the wavelength of light is usually much longer than the atomic lattice parameter. The symmetry analysis is supported by the calculations of the microscopic model below.

Model. We start with a strongly correlated electronic model for transition metal (TM) compounds forming an edge-sharing octahedral geometry [as shown by black circles in Fig. 1(a)]. In this class of materials, the d orbital forms an octahedral geometry with the p -block (ligand) elements [chalcogenic or halogenic atoms; see green circles in Fig. 1(b)]. Depending on the electronic configuration of the d -block elements, such compounds can be modeled by either the single- or the multiorbital Hubbard model [31]. A circularly polarized light [see Fig. 1(a)] is applied which modifies the hopping between different orbitals. For a typical single-orbital model, the Hamiltonian can be written as $\mathcal{H}(t) = \mathcal{H}_0 + \mathcal{H}_1(t)$, where

$$\mathcal{H}_0 = U \sum_i n_{i\uparrow}^d n_{i\downarrow}^d + \Delta \sum_{i,\sigma} p_{i\sigma}^\dagger p_{i\sigma}, \quad (1a)$$

$$\mathcal{H}_1(t) = \sum_{\langle ij \rangle} [t_{pd}^{ij}(t) d_{i\uparrow}^\dagger p_{j\sigma} + t_{\sigma\sigma'}^{ij}(t) d_{i\sigma}^\dagger d_{j\sigma'}] + \text{H.c.}, \quad (1b)$$

where U denotes the onsite Coulomb repulsion of the d orbital and Δ parameterizes the ligand charge transfer energy. Note that we consider only one d orbital along with the ligand p orbital. Here we assume the sum over repeated spin indices σ , and $t_{pd}^{ij}(t)$ and $t_{\sigma\sigma'}^{ij}(t)$ are the time-dependent hopping amplitudes between p and d and two d orbitals, respectively. In the presence of circularly polarized light with electric-field component $\mathbf{E}(t) = E_0(-\hat{\mathbf{x}} \cos \Omega t + \hat{\mathbf{y}} \sin \Omega t)$, the hopping depends on Peierls phase as (we work in the unit of $e, \hbar, c = 1$)

$$t_{pd}^{ij}(t) = t_{pd} e^{i\theta_{ij}(t)}, \quad \theta_{ij}(t) = -\mathbf{r}_{pd} \cdot \mathbf{A}(t), \quad (2a)$$

$$t_{\sigma\sigma'}^{ij}(t) = [t_{dd} \mathbb{I}_2 + i\boldsymbol{\alpha}_{ij} \cdot \boldsymbol{\tau}]_{\sigma\sigma'} e^{i\phi_{ij}(t)}, \quad (2b)$$

$$\phi_{ij}(t) = -\mathbf{r}_{dd} \cdot \mathbf{A}(t), \quad (2c)$$

where the vector potential $\mathbf{A}(t) = \frac{E_0}{\Omega}(\hat{\mathbf{x}} \sin \Omega t + \hat{\mathbf{y}} \cos \Omega t)$, $\boldsymbol{\tau}$ denotes the vector of Pauli matrices, $\boldsymbol{\alpha}_{ij} = (\alpha_{ij}^1, \alpha_{ij}^2, \alpha_{ij}^3)$ is a real vector corresponding to the strength of the SOC in the d - d bond, and \mathbf{r}_{pd} and \mathbf{r}_{dd} are the nearest-neighbor vectors between p and d and two d orbitals, respectively. The specific form of the SOC in Eq. (2b) dictates that the Hamiltonian in Eq. (1b) is not invariant under inversion, i.e., $\mathcal{I}\mathcal{H}_1(t)\mathcal{I}^{-1} \neq \mathcal{H}_1(t)$. Here \mathcal{I} is the inversion operator which swaps the indices i and j . We consider the insulating regime at half filling with $U, \Delta \gg t_{pd}, t_{dd}, |\boldsymbol{\alpha}|$. Our analysis does not require the energy hierarchy between U and Δ and therefore is valid both for the Mott and for the charge-transfer type insulator. We broadly term the insulator as the Mott insulator in the following discussions. The presence of $\boldsymbol{\alpha}_{ij}$ violates the inversion symmetry but preserves the TRS when the laser is off $\mathbf{A} = 0$.

Starting from the Hamiltonian in Eqs. (1a) and (1b), we go to the rotated frame as $\mathcal{H}_{\text{rot}}(t) = e^{i\mathcal{S}(t)}[\mathcal{H}(t) - i\partial_t]e^{-i\mathcal{S}(t)}$, where $\mathcal{S}(t)$ is a Hermitian operator. Writing $\mathcal{S}(t) = \mathcal{S}^{(1)}(t) + \mathcal{S}^{(2)}(t) + \dots$ and expanding $\mathcal{H}_{\text{rot}}(t)$ in Taylor series, we obtain order-by-order low-energy effective spin-exchange Hamiltonians. For the subsequent analysis, we consider a simplified four-site cluster model [see Fig. 1(b)] containing two d orbitals and two ligand atoms. In the large frequency approximation ($\Omega \gg t_{pd}, t_{dd}, \alpha_{ij}$), we obtain an effective low-energy spin Hamiltonian up to third order in perturbation theory as (see Supplemental Material (SM) [32])

$$\mathcal{H}_{\text{eff}} = \sum_{\langle ij \rangle} [\mathbf{S}_{i\mu} \Gamma_{\mu,\nu} \mathbf{S}_{j\nu} + \mathbf{h}_{ij}^{\text{eff}} \cdot (\mathbf{S}_i - \mathbf{S}_j)]. \quad (3)$$

The results for the exchange couplings $\Gamma_{\mu,\nu}$ ($\mu, \nu = x, y, z$) are provided in the SM [32]. In the absence of the SOC and the ligand atoms, we recover the well-known Floquet Hamiltonian $\mathcal{H}_{\text{eff}} = \sum_{\langle ij \rangle} J_{ij} \mathbf{S}_i \cdot \mathbf{S}_j$, where $J_{ij} = 4 \sum_n \mathcal{J}_n^2(A_0) t_{dd}^2 / (U - n\Omega)$, $\mathcal{J}_n(x)$ is the Bessel function of the first kind and $A_0 = r_{dd} E_0 / \Omega$ [29,33,34].

The magnetic-field term $\mathbf{h}_{ij}^{\text{eff}}$ is evaluated as

$$\mathbf{h}_{ij}^{\text{eff}} = \sum \frac{8 \mathcal{J}_n(A_0) \mathcal{J}_m(A) \mathcal{J}_l(A) t_{pd}^2 \boldsymbol{\alpha}_{ij}}{3[\Delta + l\Omega][U - n\Omega]} \sin \psi_0^{ml}, \quad (4)$$

where \sum signifies summation over the indices n, m, l with the constraint $n + m + l = 0$, $A_0 = r_{dd} E_0 / \Omega$, $A = r_{pd} E_0 / \Omega$, and $\psi_0^{ml} = (m - l)\psi_0$. Here ψ_0 is the angle between p - d - and d - d -orbital bonds [see Fig. 1(b)]. Note that the effective magnetic-field $\mathbf{h}_{ij}^{\text{eff}}$ proportional to the SOC $\boldsymbol{\alpha}_{ij}$ is a consequence of the

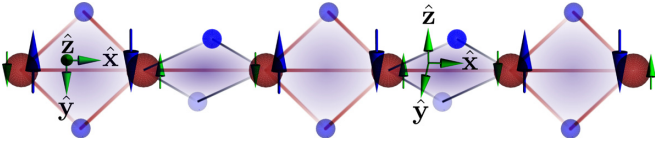


FIG. 2. A schematic of the proposed distorted lattice structure where two consecutive (neighboring) four-site clusters of atoms are rotated relatively along the x axis. The circularly polarized light is shined normal to the unrotated x - y plane. Big red atoms signify the d orbital and the smaller blue atoms correspond to the ligand site. The spin arrangement (big arrows) on a perfectly aligned (in the xy plane) cluster is oriented along the z axis, whereas the neighboring cluster tilted along the z axis leads to a tilted spin arrangement which has a smaller z component (smaller arrow). The IFE favors an antiferromagnetic order along the chain.

broken time-reversal symmetry due to the applied circularly polarized light. Since the effective magnetic field couples to $(\mathbf{S}_i - \mathbf{S}_j)$, it favors an antiferromagnetic static magnetization, which is consistent with the symmetry analysis.

For a weak laser drive and low frequency, the static magnetic field due to IFE is proportional to square of the electric field and inversely proportional to the frequency. Its [see Eq. (4)] asymptotic form is given by

$$\mathbf{h}_{ij}^{\text{eff}} \approx \frac{4t_{pd}^2 \alpha_{ij}}{3\Omega} \frac{E_0^2 r_{pd} \sin \psi_0}{U \Delta^2} (2r_{pd} \cos \psi_0 + r_{dd}), \quad (5)$$

which matches qualitatively with our phenomenological ansatz. However, as $\mathbf{h}_{ij}^{\text{eff}}$ couples antiferromagnetically to the localized spins on the d -orbital sites, the net magnetization would vanish if all the consecutive four-site clusters are aligned parallel to the xy plane, whereas if the neighboring clusters are tilted along the z axis, the emergent Zeeman magnetic field would point in two different directions as illustrated in Fig. 2. In this case, the net magnetization on a particular site (d orbital) would not be zero and this antiferromagnetic order induced by the IFE can be realized in broken inversion symmetric systems. The variation of h^{eff} , at the laser frequency $\Omega = 10$ eV, is illustrated in Fig. 3(a) for a set of generic parameters.

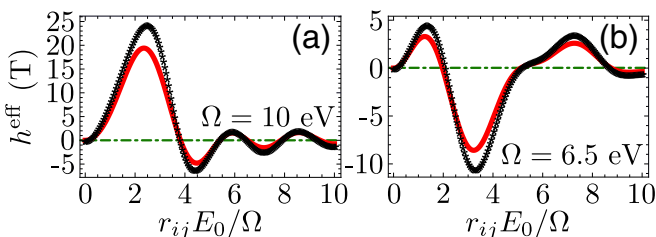


FIG. 3. Dependence solid line, perturbation calculations; symbols, exact diagonalization results (see SM [32]) of the IFE magnetic field due to the circularly polarized light for (a) the single-orbital case [Eq. (4)] and (b) the multi-orbital case [Eq. (9)]. For the single-orbital case, we use generic material parameters as $U = 8$ eV, $\Delta = 16$ eV, $t_{dd} = 1.0$ eV, $t_{pd} = 1.5$ eV, and $\alpha_{ij}^3 = 0.05$ eV, whereas we adopt the material parameters for α -RuCl₃ [47,48] in panel (b). Here we assume g -factor $g = 2$ and plot the amplitude of $\mathbf{h}_{ij}^{\text{eff}}$.

Multiorbital model. In this case, we consider an inversion symmetric system and necessarily adopt a multiorbital description with atomic SOC. For subsequent analysis, we focus on the Kitaev systems such as α -RuCl₃, β -Li₂IrO₃ where five electrons reside in the t_{2g} manifold of the TM d orbital [see Fig. 1(a)], which further splits into $j_{\text{eff}} = 1/2$ and $j_{\text{eff}} = 3/2$ states due to strong SOC [35–41]. For d^5 -electronic configuration, the $j_{\text{eff}} = 3/2$ manifold is completely filled and a lone electron henceforth resides on the $j_{\text{eff}} = 1/2$ manifold. The electronic model to capture the effects of SOC and the charge transfer to the ligand p orbitals is written in terms of the Kanamori Hamiltonian [42–44] as

$$\begin{aligned} \mathcal{H}_0 = & U \sum_{i\alpha} n_{i\alpha,\uparrow}^d n_{i\alpha,\downarrow}^d + \sum_{i\sigma\sigma'\alpha\neq\beta} (U' - \delta_{\sigma\sigma'} J_H) n_{i\alpha\sigma}^d n_{i\beta\sigma'}^d \\ & + J_H \sum_{i\alpha\neq\beta} (d_{i\alpha\uparrow}^\dagger d_{i\alpha\downarrow}^\dagger d_{i\beta\downarrow} d_{i\beta\uparrow} + d_{i\alpha\uparrow}^\dagger d_{i\beta\downarrow}^\dagger d_{i\alpha\downarrow} d_{i\beta\uparrow}) \\ & + \frac{\lambda}{2} \sum_i d_i^\dagger (\mathbf{L} \cdot \mathbf{S}) d_i + \Delta \sum_{i\sigma} n_{i\sigma}^p, \end{aligned} \quad (6)$$

where U, U' denote the intra- and interorbital Coulomb repulsions and J_H stands for the Hund's coupling between the three t_{2g} orbitals: $d_{xy}, d_{yz},$ and d_{zx} . Here Δ , as before, denotes the ligand charge-transfer energy and λ is the strength of the SOC.

Assuming SOC strength λ is much smaller compared with the other parameters as $U, \Delta, \Omega \gg \lambda$, the Kanamori Hamiltonian can be rewritten in terms of the irreducible representation of the doubly occupied states in the d orbital [32,45,46] as

$$\mathcal{H}_0 = \sum_i \sum_{\Gamma} \sum_{g_{\Gamma}} U_{\Gamma} |i; \Gamma, g_{\Gamma}\rangle \langle i; \Gamma, g_{\Gamma}| + \Delta \sum_{i\sigma} n_{i\sigma}^p, \quad (7)$$

where Γ corresponds to the particular irreducible representation and g_{Γ} characterizes the degeneracy of that state. The total energy of the four different nondegenerate states is given [46] as $U_{A_1} = U + 2J_H$, $U_E = U - J_H$, $U_{T_1} = U - 3J_H$, and $U_{T_2} = U - J_H$.

Next, we evaluate the hopping Hamiltonian based on the inherent symmetries of the octahedral geometry. The Hamiltonian in the presence of circularly polarized light is written as

$$\begin{aligned} \mathcal{H}_1(t) = & \sum_{ij,\sigma} e^{i\phi_{ij}(t)} [d_{ixz\sigma}^\dagger d_{iyz\sigma}^\dagger d_{ixy\sigma}^\dagger] \begin{bmatrix} t_1 & t_2 & t_4 \\ t_2 & t_1 & t_4 \\ t_4 & t_4 & t_3 \end{bmatrix} \begin{bmatrix} d_{jxz\sigma} \\ d_{jyz\sigma} \\ d_{jxy\sigma} \end{bmatrix} \\ & + t_{pd} \sum_{ij\sigma} [e^{i\theta_{ij}(t)} p_{i\sigma}^\dagger d_{jyz\sigma} + e^{i\theta_{ij}(t)} p_{j\sigma}^\dagger d_{iyz\sigma} \\ & + e^{i\theta_{ij}(t)} d_{jxz\sigma}^\dagger p_{i\sigma} + e^{i\theta_{ij}(t)} d_{jxz\sigma}^\dagger p_{j\sigma}^\dagger] + \text{H.c.}, \end{aligned} \quad (8)$$

where $p_{i\sigma}^\dagger$ is the creation operator at the ligand sites, surrounding the TM orbitals, and $\phi_{ij}(t)$ and $\theta_{ij}(t)$ denote the bond-angle-dependent Peierls phases. For the multiorbital analysis, we adopt all the parameters entering Eq. (6) and Eq. (7) from the recent *ab initio* [47] and photoemission reports [48] for α -RuCl₃ as $U = 3.0$ eV, $J_H = 0.45$ eV, $\Delta = 5$ eV, $t_1 = 0.036$ eV, $t_2 = 0.191$ eV, $t_3 = -0.062$ eV, $t_4 = -0.024$ eV, and $t_{pd} = -0.9$ eV.

We employ a similar time-dependent SW transformation and evaluate the low-energy effective spin model up to third order in perturbation. In the high-frequency approximation, the effective Hamiltonian is obtained as $\mathcal{H}_{\text{eff}} = \sum_{(ij)} \mathbf{S}_{i\mu} \mathcal{M}_{i\mu,j\nu} \mathbf{S}_{j\nu} + \sum_{(ij)} \mathbf{h}_{ij}^{\text{eff}} \cdot (\mathbf{S}_i + \mathbf{S}_j)$, where $\mu, \nu = x, y, z$. The magnetic interactions $\mathcal{M}_{i\mu,j\nu}$ (the expressions are shown in the SM [32,49]) can be controlled by laser, which imply a promising route to stabilize quantum spin liquid by tuning the competing interactions in favor of the quantum spin liquid [36,50–52]. Here we focus on the photo-induced emergent magnetic-field $\mathbf{h}_{ij}^{\text{eff}}$, which is written in terms of the model parameters as

$$\mathbf{h}_{ij}^{\text{eff}} = \sum \frac{8\mathcal{J}_n(A_0)\mathcal{J}_m(A)\mathcal{J}_l(A)t_{pd}^2 \sin \psi_0^{ml}}{27 \Delta + l\Omega} \times \left[\frac{t_1 - t_3}{U - 3J_H - n\Omega} + \frac{t_1 - t_3}{U - J_H - n\Omega} \right] \hat{\mathbf{z}}, \quad (9)$$

where \sum signifies summation over the indices n, m, l with the constraint $n + m + l = 0$, $A_0 = r_{dd}E_0/\Omega$, $A = r_{pd}E_0/\Omega$, and $\psi_0^{ml} = (m - l)\psi_0$. In contrast with the single-orbital case, the effective Zeeman magnetic field couples to the symmetric combination of the spins ($\mathbf{S}_i + \mathbf{S}_j$). Consequently, the applied polarized light generates a ferromagnetic magnetization in this case, which was also studied for α -RuCl₃ in Ref. [52] recently using numerical exact diagonalization. Here we *emphasize* that our analysis is applicable to a wider class of Mott insulators with inversion symmetry.

For weak laser drive and low frequency, $\mathbf{h}_{ij}^{\text{eff}}$ can be expanded asymptotically as

$$\mathbf{h}_{ij}^{\text{eff}} \approx \frac{4t_{pd}^2(t_1 - t_3) E_0^2 r_{pd} \sin \psi_0}{27\Omega \Delta^2} (2r_{pd} \cos \psi_0 + r_{dd}) \times \left(\frac{1}{U - 3J_H} + \frac{1}{U - J_H} \right). \quad (10)$$

Since the TM atoms in the α -RuCl₃ unit cell lie in the mirror plane and have additional inversion symmetry, this result is consistent with our phenomenological ansatz. The variation of $\mathbf{h}_{ij}^{\text{eff}}$ with the laser drive is shown in Fig. 3(b) for $\Omega = 6.5$ eV.

Discussion and conclusion. In this work we use the Floquet theory to study the IFE in Mott insulators. The Floquet formulation allows us to study the strong drive region systematically that goes beyond the weak drive results known before, i.e., the induced IFE Zeeman field $\mathbf{h}_{\text{IFE}} \propto \mathbf{E}(\Omega) \times \mathbf{E}^*(\Omega)$. It also informs the heating associated with IFE due to laser irradiation. Our results are valid in the Floquet prethermal region, which can be exponentially long in time before the system evolves into the infinite temperature state if the laser frequency is tuned away from resonances of the system [53–64]. The resonances in our models include the resonances in the Hubbard gap, the charge transfer gap, the crystal-field splitting gap, and the spin-orbit splitting gap of the j_{eff} multiplets. The IFE is resonantly enhanced near resonances in a short-time scale,

but heating quickly dominates, which invalidates the Floquet description. The IFE magnetic field can be of the order of 10 Tesla even away from the resonances.

We proposed a toy model (see Fig. 2) to demonstrate the antiferromagnetic order favored by the IFE in materials with broken inversion symmetry. Certain distorted layered honeycomb compounds, such as Li₃Cu₂SbO₆ [65], can also realize our prediction. The single-orbital model can be realized in similar lattice geometries with a d^9 -electronic configuration. The SOC can be induced by placing the thin films atop a substrate with heavy ions. To clearly distinguish the antiferromagnetic order induced by IFE from the antiferromagnetic Heisenberg exchange interaction, experiments can be performed above the magnetic ordering temperature. Below the ordering temperature a competition between the spin-exchange couplings and the induced magnetic field $\mathbf{h}_{ij}^{\text{eff}}$ can stabilize complex magnetic orders.

We specifically focused on a d^5 -electronic configuration in edge-sharing octahedral structure for the IFE in the multi-orbital systems. Throughout the analysis, we assumed a perpendicular incidence of light polarization to the TM-ligand-TM atom plane. Apart from the laser amplitude and frequency, the angle between the light polarization and the TM-ligand-TM atom plane, for an oblique incidence, provides yet another tunability to control the spin-exchange couplings and the overall sign of both ferro- and antiferromagnetic IFE Zeeman field [32]. By choosing the incident angle, we can stabilize an antiferromagnetic order using the IFE by avoiding a complete cancellation of the IFE Zeeman field between neighboring clusters.

To summarize, we studied the IFE in Mott insulators irradiated by a circularly polarized light. Based on both the symmetry consideration and the microscopic model calculations using the Floquet theory, we showed that the IFE in Mott insulators without (with) inversion symmetry favor antiferromagnetic (ferromagnetic) order. Our results suggest a promising route to ultrafast control of magnetic order in Mott insulators by light.

Note added. We recently became aware of an experiment [66] where a similar *antiferromagnetic* coupling of response functions (polarization) to neighboring spins is observed in a periodically driven *noncentrosymmetric* Mott insulator (MnPS₃).

Acknowledgments. We thank Avadh Saxena, Alexander V. Balatsky, and Dieter Vollhardt for providing important feedback while writing this paper and thank Nicholas Sirica, Rohit Prasankumar, Sang-Wook Cheong, and Jianxin Zhu for the helpful discussions. This work was carried out under the auspices of the U.S. Department of Energy (DOE), National Nuclear Security Administration under Contract No. 89233218CNA000001 through the LDRD Program. S.Z.L. was also supported by the U.S. DOE, Office of Science, Basic Energy Sciences, Materials Sciences and Engineering Division, Condensed Matter Theory Program.

- [1] A. Kirilyuk, A. V. Kimel, and T. Rasing, *Rev. Mod. Phys.* **82**, 2731 (2010).
 [2] P. Forn-Díaz, L. Lamata, E. Rico, J. Kono, and E. Solano, *Rev. Mod. Phys.* **91**, 025005 (2019).

- [3] P. N. Schatz and A. J. McCaffery, *Q. Rev. Chem. Soc.* **23**, 552 (1969).
 [4] L. P. Pitaevskii, *JETP* **12**, 1008 (1961).

- [5] J. P. van der Ziel, P. S. Pershan, and L. D. Malmstrom, *Phys. Rev. Lett.* **15**, 190 (1965).
- [6] A. V. Kimel, A. Kirilyuk, P. A. Usachev, R. V. Pisarev, A. M. Balbashov, and T. Rasing, *Nature (London)* **435**, 655 (2005).
- [7] T. Lottermoser, T. Lonkai, U. Amann, D. Hohlwein, J. Ihinger, and M. Fiebig, *Nature (London)* **430**, 541 (2004).
- [8] M. B. Jungfleisch, Q. Zhang, W. Zhang, J. E. Pearson, R. D. Schaller, H. Wen, and A. Hoffmann, *Phys. Rev. Lett.* **120**, 207207 (2018).
- [9] Y. Gu and K. G. Kornev, *J. Opt. Soc. Am. B* **27**, 2165 (2010).
- [10] R. Hertel, *J. Magn. Magn. Mater.* **303**, L1 (2006).
- [11] S. R. Woodford, *Phys. Rev. B* **79**, 212412 (2009).
- [12] C. A. Perroni and A. Liebsch, *Phys. Rev. B* **74**, 134430 (2006).
- [13] M. Battiato, G. Barbalinardo, and P. M. Oppeneer, *Phys. Rev. B* **89**, 014413 (2014).
- [14] Y. Tanaka, T. Inoue, and M. Mochizuki, *New J. Phys.* **22**, 083054 (2020).
- [15] Y. Gao, C. Wang, and D. Xiao, [arXiv:2009.13392](https://arxiv.org/abs/2009.13392).
- [16] I. D. Tokman, Q. Chen, I. A. Shereshevsky, V. I. Pozdnyakova, I. Oladyshev, M. Tokman, and A. Belyanin, *Phys. Rev. B* **101**, 174429 (2020).
- [17] L. Liang, P. O. Sukhachov, and A. V. Balatsky, *Phys. Rev. Lett.* **126**, 247202 (2021).
- [18] S. V. Mironov, A. S. Mel'nikov, I. D. Tokman, V. Vadimov, B. Lounis, and A. I. Buzdin, *Phys. Rev. Lett.* **126**, 137002 (2021).
- [19] A. H. Majedi, *Phys. Rev. Lett.* **127**, 087001 (2021).
- [20] P. Němec, M. Fiebig, T. Kampfrath, and A. V. Kimel, *Nat. Phys.* **14**, 229 (2018).
- [21] E. Paris, C. W. Nicholson, S. Johnston, Y. Tseng, M. Rumo, G. Coslovich, S. Zohar, M. F. Lin, V. N. Strocov, R. Saint-Martin, A. Revcolevschi, A. Kemper, W. Schlotter, G. L. Dakovski, C. Monney, and T. Schmitt, *npj Quantum Mater.* **6**, 51 (2021).
- [22] A. V. Kimel and A. K. Zvezdin, *Low Temp. Phys.* **41**, 682 (2015).
- [23] A. V. Kimel, B. A. Ivanov, R. V. Pisarev, P. A. Usachev, A. Kirilyuk, and T. Rasing, *Nat. Phys.* **5**, 727 (2009).
- [24] J. A. de Jong, A. V. Kimel, R. V. Pisarev, A. Kirilyuk, and T. Rasing, *Phys. Rev. B* **84**, 104421 (2011).
- [25] A. I. Popov, K. A. Zvezdin, Z. V. Gareeva, A. V. Kimel, and A. K. Zvezdin, *Phys. Rev. B* **103**, 014423 (2021).
- [26] J. R. Schrieffer and P. A. Wolff, *Phys. Rev.* **149**, 491 (1966).
- [27] A. B. Harris and R. V. Lange, *Phys. Rev.* **157**, 295 (1967).
- [28] M. Bukov, M. Kolodrubetz, and A. Polkovnikov, *Phys. Rev. Lett.* **116**, 125301 (2016).
- [29] U. Kumar and S.-Z. Lin, *Phys. Rev. B* **103**, 064508 (2021).
- [30] T. Moriya, *Phys. Rev.* **120**, 91 (1960).
- [31] M. Imada, A. Fujimori, and Y. Tokura, *Rev. Mod. Phys.* **70**, 1039 (1998).
- [32] See Supplemental Material at <http://link.aps.org/supplemental/10.1103/PhysRevB.105.L180414> for the all the details of the Floquet SW transformation to derive the low-energy spin model. .
- [33] J. H. Mentink, K. Balzer, and M. Eckstein, *Nat. Commun.* **6**, 6708 (2015).
- [34] M. Eckstein, J. H. Mentink, and P. Werner, [arXiv:1703.03269](https://arxiv.org/abs/1703.03269).
- [35] J. A. Sears, M. Songvilay, K. W. Plumb, J. P. Clancy, Y. Qiu, Y. Zhao, D. Parshall, and Y.-J. Kim, *Phys. Rev. B* **91**, 144420 (2015).
- [36] G. Jackeli and G. Khaliullin, *Phys. Rev. Lett.* **102**, 017205 (2009).
- [37] J. Chaloupka, G. Jackeli, and G. Khaliullin, *Phys. Rev. Lett.* **110**, 097204 (2013).
- [38] J. G. Rau, E. K.-H. Lee, and H.-Y. Kee, *Phys. Rev. Lett.* **112**, 077204 (2014).
- [39] S. M. Winter, Y. Li, H. O. Jeschke, and R. Valentí, *Phys. Rev. B* **93**, 214431 (2016).
- [40] S. M. Winter, A. A. Tsirlin, M. Daghofer, J. van den Brink, Y. Singh, P. Gegenwart, and R. Valentí, *J. Phys.: Condens. Matter* **29**, 493002 (2017).
- [41] D. Gotfryd, J. Rusnačko, K. Wohlfeld, G. Jackeli, J. Chaloupka, and A. M. Oleś, *Phys. Rev. B* **95**, 024426 (2017).
- [42] J. Kanamori, *Prog. Theor. Phys.* **17**, 177 (1957).
- [43] J. Kanamori, *Prog. Theor. Phys.* **17**, 197 (1957).
- [44] A. Georges, L. d. Medici, and J. Mravlje, *Annu. Rev. Condens. Matter Phys.* **4**, 137 (2013).
- [45] S. Ishihara, T. Hatakeyama, and S. Maekawa, *Phys. Rev. B* **65**, 064442 (2002).
- [46] N. Arakawa, *Phys. Rev. B* **94**, 174416 (2016).
- [47] H.-S. Kim and H.-Y. Kee, *Phys. Rev. B* **93**, 155143 (2016).
- [48] S. Sinn, C. H. Kim, B. H. Kim, K. D. Lee, C. J. Won, J. S. Oh, M. Han, Y. J. Chang, N. Hur, H. Sato, B.-G. Park, C. Kim, H.-D. Kim, and T. W. Noh, *Sci. Rep.* **6**, 39544 (2016).
- [49] U. Kumar, S. Banerjee, and S.-Z. Lin, [arXiv:2111.01316](https://arxiv.org/abs/2111.01316).
- [50] J. G. Rau, E. K.-H. Lee, and H.-Y. Kee, *Annu. Rev. Condens. Matter Phys.* **7**, 195 (2016).
- [51] N. Arakawa and K. Yonemitsu, *Phys. Rev. B* **103**, L100408 (2021).
- [52] A. Sriram and M. Claassen, [arXiv:2105.01062](https://arxiv.org/abs/2105.01062).
- [53] S. A. Weidinger and M. Knap, *Sci. Rep.* **7**, 45382 (2017).
- [54] F. Machado, G. D. Kahanamoku-Meyer, D. V. Else, C. Nayak, and N. Y. Yao, *Phys. Rev. Research* **1**, 033202 (2019).
- [55] K. Hejazi, J. Liu, and L. Balents, *Phys. Rev. B* **99**, 205111 (2019).
- [56] A. Haldar, R. Moessner, and A. Das, *Phys. Rev. B* **97**, 245122 (2018).
- [57] D. A. Abanin, W. De Roeck, and F. Huveneers, *Phys. Rev. Lett.* **115**, 256803 (2015).
- [58] T. Mori, T. Kuwahara, and K. Saito, *Phys. Rev. Lett.* **116**, 120401 (2016).
- [59] D. A. Abanin, W. De Roeck, W. W. Ho, and F. Huveneers, *Phys. Rev. B* **95**, 014112 (2017).
- [60] D. V. Else, B. Bauer, and C. Nayak, *Phys. Rev. X* **7**, 011026 (2017).
- [61] F. Peronaci, M. Schiró, and O. Parcollet, *Phys. Rev. Lett.* **120**, 197601 (2018).
- [62] A. Herrmann, Y. Murakami, M. Eckstein, and P. Werner, *Europhys. Lett.* **120**, 57001 (2017).
- [63] T. N. Ikeda and M. Sato, *Sci. Adv.* **6**, eabb4019 (2020).
- [64] T. N. Ikeda and A. Polkovnikov, *Phys. Rev. B* **104**, 134308 (2021).
- [65] A. Bhattacharyya, T. K. Bhowmik, D. T. Adroja, B. Rahaman, S. Kar, S. Das, T. Saha-Dasgupta, P. K. Biswas, T. P. Sinha, R. A. Ewings, D. D. Khalyavin, and A. M. Strydom, *Phys. Rev. B* **103**, 174423 (2021).
- [66] J.-Y. Shan, M. Ye, H. Chu, S. Lee, J.-G. Park, L. Balents, and D. Hsieh, *Nature (London)* **600**, 235 (2021).